Langerhans Cell Histiocytosis in the Skull: Comparison of MR Image and Other Images

Soo Jin Lim[1], Myung Kwan Lim[1], Sun Won Park[1], Jung Eun Kim[1], Ji Hye Kim[2], Deok Hwan Kim[3], Seok Lyong Lee[4], Chang Hae Suh[1]

Purpose : To evaluate the characteristic MR imaging findings of Langerhans cell histiocytosis (LCH) in the skull and to compare them with those of plain radiography and computed tomography.

Materials and Methods : A total of 10 lesions in 9 patients (Age range; 5–42 years, Mean age; 18, all women) with Langerhans cell histiocytosis in the skull were included in our study. Nine lesions in nine patients were histologically confirmed by surgery or fine needle aspiration biopsy. All patients performed with MRI, and plain radiography and CT scan were done in 7 patients (8 lesions). Two experienced neuroradiologists reviewed the radiological examinations independently with attention to location, size, shape and nature of the lesions in the skull and compared the extent and extension of the lesions to adjacent structures.

Results : The lesions were distributed in all of the skulls without predilection site. On MRI, the masses were shown as well-enhancing soft tissue masses (10/10) mainly in diploic spaces (8/10) with extension to scalp (9/10) and dura mater (7/10). Dural enhancement (7/10) and thickening (4/10) were seen. The largest diameter of the soft tissue masses ranged 1.1 cm to 6.8 cm, shaped as round (5/10) or oval (5/10). On CT scans, the lesions were presented as soft tissue masses involving diploic space (6/8) and scalp extension (7/8) were also well visualized. Although bony erosion or destruction was more clearly seen on CT rather than those of MRI, enhancement of soft tissue masses and dura were not well visualized on CT. In contrast, all of the lesions in LCH were seen as punched out (4/8), beveled-edge appearance (4/8) osteolytic masses in plain radiography, but scalp and dural extension could not be seen.

Conclusion : Characteristic MR findings in patients with LCH are soft tissue mass in diploic space with extension to dura and scalp, and MRI would be better imaging modality than plain radiography or CT .

Index words : Langerhans cell histiocytosis
Skull
Computed tomography (CT)
Magnetic resonance (MR)

JKSMRM 13:74-80(2009)

[1]Department of Radiology, Inha University, College of Medicine, [2]Sungkyunkwan University, Samsung Medical Center,
[3]Department of Electronic Engineering, Inha University,
[4]School of Industrial and Management Eng. Hankuk University of Foreign Studies

This work was supported by the Korea Science and Engineering Foundation (KOSEF) grant funded by the Korea government(MEST) (R01-2008-000-20685-0).

Received; April 26, 2009, revised; May 5, 2009, accepted; May 23, 2009

Corresponding author : Myung Kwan Lim, M.D., Department of Radiology, Inha University Hospital
7-206, 3-ga, Shinheung-dong, Choong-gu, Incheon 400-711, Korea.
Tel. 82-32-890-2769 Fax. 82-32-890-2743 E-mail: kanlim@inha.ac.kr

Introduction

Langerhans cell histiocytosis (LCH) is a rare disease and regarded as a reactive clonal disease of the monocyte-macrophage system and may affect almost any organ (1, 2). The radiologic presentations of LCH are variable and range from a lytic skeletal lesion incidentally seen at radiography to widespread disease with severe organ dysfunction (3). Bony lesions are the most common manifestation of LCH and the skull is most frequently involved (4).

It is well known that most bony lesions can be detected on plain radiographs as punched out lesion and CT or MR images can be helpful in providing better delineation of the bony lesion (5). However, precise CT and MR imaging findings are not well documented in previous studies and no comparative trials that demonstrated the clear advantage of one imaging modality over the other one have been reported, to our knowledge. The purpose of this report is to describe imaging findings of MRI in LCH patients with skull involvement and to compare them with those of plain radiographs and CT scans.

Materials and Methods

A total of 27 patients with LCH in the skull were suspected at two major university hospitals . Among them, 10 lesions in 9 patients (a patient had 2 lesions) were histologically confirmed by surgery (4/9) or fine needle aspiration (5/9). The age distribution of these patients was 5–42 years (mean age, 18 years), and all patients were female. The chief complaint of the 5 patient was

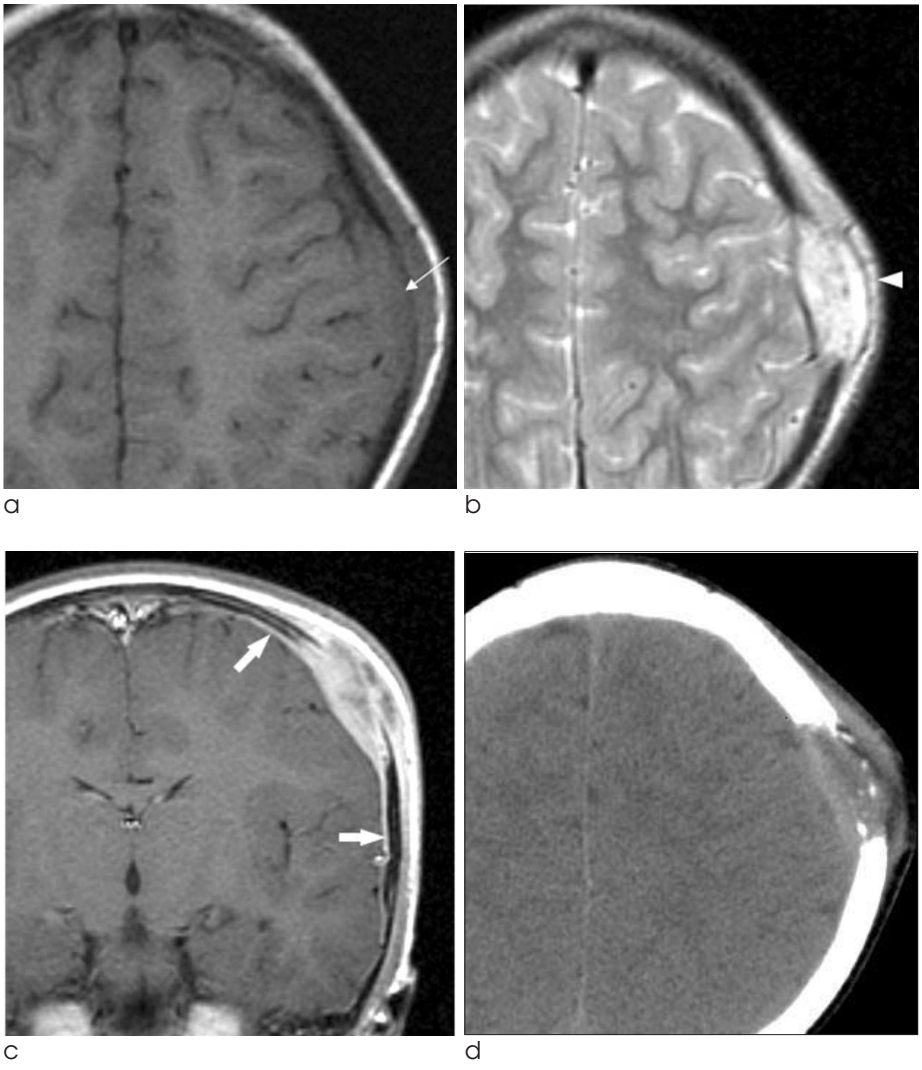

Fig 1. a-d. A 29-year-old woman with LCH.
Axial T1-weighted (a) and T2-weighted images (b) show iso (arrow) and high signal intensity (arrow head) of the mass. MR images also show osteolysis of the skull and extension of the mass to the scalp. Coronal contrast-enhanced T1-weighted image (c) shows strong enhancement of the mass. Adjacent dural thickening and enhancement (arrows) is clearly seen on this image.
Axial contrast-enhanced CT scan (d) shows well-enhancing osteolytic mass in left frontal bone. Extracranial extension of the soft tissue mass is clearly seen.

scalp swelling , and the others were palpable mass. All patients performed with MRI, but simple skull X-ray and CT scan were done in 7 patients (8 lesions).

A typical brain CT examination (Somatom Sensation 16; Siemens Medical Systems, Erlangen, Germany) had been performed in the axial planes from the skull vault to skull base. Sections were 5-mm thick and contiguous, and images were obtained after the intravenous administration of 60–120 ml of non-ionic contrast medium (Ultravist [iopramide]; Schering, Berlin, Germany).

Brain MR imaging was performed with a 1.5 T MR scanner (Signa HDx; GE Medial Systems, Milwaukee, Wisconsin, U.S.A.). We acquired axial T2- and T1-weighted images and contrast-enhanced axial and coronal T1-weighted images using the following parameters: for T2-weighted images, TR were 2200– 4600 ms and TE was 90–110 ms; for T1-weighted images, TR was 400–600 ms and TE was 10–20 ms; section thickness, 5.0 mm; FOV, 240 × 240 mm; and matrix, 256 × 256. Gadodiamide (Omniscan, 0.2 mmol/kg; Nycomed, Norway) was administered.

Two experienced neuroradiologist reviewed the radiologic examinations retrospectively, with attention to location, size, shape and nature of the lesions in the skull on all plain radiographs, CT and MR imaging. The involving layers including adjacent dura, attenuation or signal intensity of the lesions, and presence of enhancement were also evaluated on both CT and MR images.

Results

On MR images, the lesions were distributed in all of the skull without predilection site. The most frequently involving site was the parietal bone in 4 and occipital bone in 3 cases. The size of the lesions was ranged as 1.1–6.8 cm (mean size, 3.1 cm). The lesions showed round in 5 and oval shape in 5 cases. The lesions presented as well-enhancing soft tissue mass (10/10), and mainly located in the diploic space (8/10) with extension to scalp (9/10), and dura mater (7/10). The signal intensity of the soft-tissue masses were isointense with gray matter on T1-weighted images and hyperintense on T2-weighted images in 9 lesions. In one lesion, heterogeneous signal intensity was seen in the center of mass on both T1- and T2- weighted images, which suggested hemorrhage or tumor necrosis. In 7 of 10 lesions, adjacent dura were enhanced and 4 lesions accompanied by dural thickening (Fig. 1a-c).

On CT scans, the lesions were presented as soft tissue masses involving diploic space (6/8) with scalp extension (7/8). Bony erosion and destruction were clearly seen in all patients (Fig. 1d). However, enhancement of soft tissue masses and dura or dural extension was not well visualized on CT scans.

In contrast, the lesions in LCH were seen as punched out (4/8) or beveled-edge appearance (4/8) in plain skull radiography (Fig. 2). One lesion was shown as geographic patters. Soft tissue mass or scalp and dural extension of the lesions could not be visualized on plain radiographs.

Discussion

Langerhans cell histiocytosis, previously called histio-

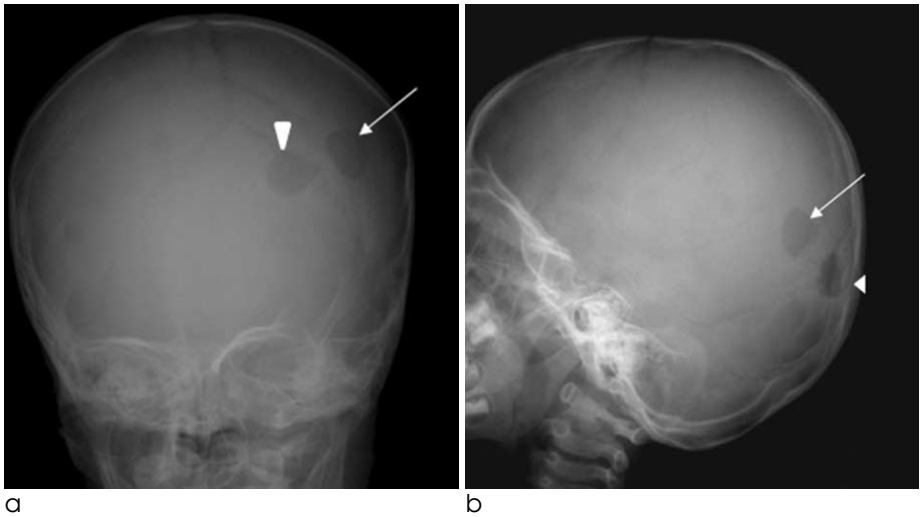

a b

Fig . 2. a, b. A 5-year-old girl with LCH.
a. Skull AP radiograph shows two rounded radiolucent lesions in left parietal (arrow) and occipital bone (arrow head). b. Lateral radiograph of the skull shows punched out lesion in parietal (arrow) and a typical beveled appearance in occipital bone (arrow head) due to unequal destruction of the inner and outer tables of the skull.

cytosis X, encompasses a spectrum of multi-system lymphoreticular disorders that predominantly affect children and young adults (5). Three overlapping clinical variants have been recognized. Letterer-Siwe disease (about 10%) is the acute fulminant form with poor prognosis; it involves skin, liver, spleen, lymph nodes, and bone primarily in children under two years of age. Hand-Schuller-Christian disease (15–40%) is the chronic form with variable prognosis; it involves skeletal, reticuloendothelial, and other visceral sites predominantly in children between five and ten years of age. Solitary or multiple eosinophilic granuloma of bone (60–80%) has a favorable prognosis; it occurs during the first three decades of life with peak incidence between five and ten years (4, 6, 7). Eosinophilic granuloma is also known to be a relatively uncommon entity, accounting for only 1% of all tumor like lesions of bone (5). In this study, all cases were eosinophilic granuloma and age ranged from 5 years to 42 years old with only one case of multiple forms.

In the literature, about 90% of patients with eosinophilic granuloma of bone present between 5 and 15 years of age, males are affected to a slightly greater degree than females (5, 8). Especially in the skull, Langerhans cell histiocytosis appears to most commonly involve the parietal bone, followed by the frontal bone (9). But LCH can arise nearly anywhere in the brain and skull. This diagnosis should always be considered when a mass arises from the bones of the face, skull base, or calvaria in children. LCH may result in masses based in the cerebral parenchyma, spinal cord, dura, or choroid plexus. Our study differs somewhat from this finding in that all patients were women and lesion distributed without predilection site in the skull. This difference is thought to be due to the small number of cases in this study.

In our study, the most characteristic MR findings of LCH on the skull was well-enhancing soft tissue masses mostly in diploic space with extension to adjacent structures and these findings was more clearly visualized than those of the other imaging modalities. Pathologically, the soft tissue masses might be the results of with histiocytic proliferation and granuloma formation. The Langerhans cell is present in all forms of the disease, from isolated eosinophilic granuloma to Letterer- Siwe disease. The Langerhans cell is a dendritic cell of the epidermis which is characterized by a unique organelle, the Langerhans, or Birbeck granule (10, 11).

Characteristic pathologic morphology of tissue from children with LCH includes large cells with elongated, irregular nuclei, prominent nuclear grooves, folding, and indentation, moderate to abundant cytoplasm, and frequent mitotic figures (12, 13). Variable numbers of eosinophils are often present. The lesions are also characterized by osteo-clast-like multinucleated giant histiocytes with bone destruction, necrosis, hemorrhage, and eosinophilic abscesses (14, 15). In one study, osteoclast-type giant cells were found in two-thirds of cases and tended to show great variability in number (12). Also, indeterminate cells, interdigitating dendritic cells, macrophages, and T lymphocytes are often found in in-

Table 1. Clinical Data and Radiological Findings in 10 Cases of Nine Patients of LCH

No.	Age/Sex	Symptoms	Location	Size (cm)	Shape	Involving Site	Dural enhance/ thickening
1	42/F	scalp swelling	right parietal	1.1	round	diploic space, outer table, scalp	N / N
2*	5/F	palpable mass	left occipital	1.5	round	all layers†, scalp	Y / Y
3*	5/F	palpable mass	left parietal	1.5	round	all layers†, scalp	Y / Y
4	5/F	scalp swelling	left frontal	2.3	oval	outer table, scalp	N / N
5	29/F	palpable mass	left parietal	2.5	oval	all layers†, scalp	Y / Y
6	10/F	palpable mass	left frontal	3	round	outer table, scalp	N / N
7	21/F	scalp swelling	left parietal	6.8	oval	all layers†, scalp	Y / Y
8	18/F	scalp swelling	left temporal	5	round	all layers†, scalp	Y / N
9	6/F	scalp swelling	right occipital	2.5	oval	all layers†, scalp	Y / N
10	30/F	palpable mass	right occipital	3	oval	all layers†	Y / N

* same patient

† all layer : inner table, diploic space, outer table

Y : yes

N : no

creased numbers in the lesions (16, 17). Granulomas may or not be seen, and fibrosis may be seen in later lesions (18)

In almost all our cases, radiographic findings of LCH was well demarcated osteolytic lesion without sclerotic margin, so called, "punched out" lesion or beveled-edge appearance. Beveled-edge appearance is known due to the uneven destruction of the outer and inner cranial tables and also called as double-contoured appearance (4–6). Geographic pattern was seen in one our case, it was thought that the lesions may enlarge, increase in number, and coalesce to form a maplike appearance and regards as chronic form of LCH (19, 20). The plain radiographic study could not delineate the soft tissue mass or its extension which could be seen on CT or MR images at all.

CT and MR imaging may allow better demonstration of a bone lesion as well as associated soft-tissue masses in this study. We found MR imaging and CT particularly helpful in detecting and defining purely soft-tissue tumors. Calvarial lesions tend to have sharp borders with involvement of the inner and outer table of the skull, resulting in a beveled-edge appearance. MR and CT images could show not only the extent of soft tissue masses but also the extension of the masses to epidural or extrcranial site (21).

CT images could more clearly demonstrate the bony destruction of the skull than the MR images, especially the unequal destruction in the outer and inner tables. In addition, a small bony fragment near the skull defect may be seen; this suggested the presence of a button sequestrum (5). In contrast, MR imaging allow better demonstration of a soft-tissue masses as well as associated bone lesion. Involving skull layers and presence of extension to dura or scalp could be more accurately visualized on MRI than other methods. Therefore, the extent of soft tissue infiltration by LCH is best documented by MRI (and, in particular, with gadolinium- enhanced T1-weighted imaging). Moreover, dural thickening and/or enhancement are only clearly visualized on MR images.

In the literature, MR imaging is a highly sensitive, but nonspecific, modality to detect bone marrow involvement and soft tissue mass in eosinophilic granuloma (22). The lytic lesions seen on radiography and CT are low signal, or isointense to muscle, on T1-weighted images and high signal on T2-weighted images and marked enhancement after gadolinium administration (22–25). Acute lesions may also demonstrate edema of marrow, periosteum, and soft tissues (26). A dural tail can often be seen and these tails return a high signal on T2-weighted images. Healing is associated with a decrease in T2 signal intensity. Magnetic resonance imaging may be useful in the detection of an accompanying soft tissue mass or inflammation and for the demonstration of dural involvement in doubtful cases (27).

Radiographic findings of LCH in the skull often simulate other skeletal lesions, such as osteomyelitis, Ewing sarcoma, leukemia, lymphoma, and metastatic neuroblastoma (28). Because the radiological patterns in skeletal LCH are variable and may mimic those of benign and malignant conditions, CT and MR examinations should be performed after simple radiographs and have some characteristic advantages not only for diagnosis of the diseases but also evaluation of the lesion extents.

In conclusions, MR imaging might provide most useful in defining the extent of osseous disease and soft-tissue extension in the skull of patients with LCH.

References

1. A multicentre retrospective survey of Langerhans' cell histiocytosis: 348 cases observed between 1983 and 1993: The French Langerhans' Cell Histiocytosis Study Group. Arch Dis Child 1996;75:17-24
2. Arceci RJ. The histiocytoses: the fall of the Tower of Babel. Eur J Cancer 1999;35:747-767
3. Ladisch S, Jaffe ES. The histiocytoses. In: Pizzo PA, Poplack DG, eds. Principles and practice of pediatric oncology. Philadelphia, Pa: Lippincott, 1989:491-504
4. Leonidas JC. Langerhans' cell histiocytosis. In: Taveras JM, Ferrucci JM, eds. Radiology: diagnosis, imaging, intervention. Vol 5. Philadelphia: Lippincott, 1990:1-9
5. David R, Oria RA, Kumar R, et al. Radiologic features of eosinophilic granuloma of bone. AJR Am J Roentgenol 1989;153:1021-1026
6. Mirra JM. Histiocytoses. In: Mirra JM, Picci P, Gold RH, eds. Bone tumors: clinical, radiologic, and pathologic correlations. Vol 2. Philadelphia: Lea & Febiger 1989;1021-1060
7. Broadbent V, Gadner H, Komp DM, Ladisch S. Histiocytosis syndromes in children. II. Approach to the clinical and laboratory evaluation of children with Langerhans cell histiocytosis. Med Pediatr Oncol 1989;17:492-495
8. Stull MA, Kransdorf MJ, Devaney KO. From the archives of the AFIP: Langerhans cell histiocytosis of bone. Radiographics 1992;12:801-823
9. Rawlings CE 3rd, Wilkins RH. Solitary eosinophilic granuloma of the skull. Neurosurgery 1984;15:155-161

10. Favara BE, McCarthy RC, Mierau GW. Histiocytosis X. Hum Pathol 1983;14:663-676
11. Favara BE. Langerhans' cell histiocytosis pathobiology and pathogenesis. Semin Oncol 1991;18:3-7
12. Kilpatrick SE, Wenger DE, Gilchrist GS, et al. Langerhans' cell histiocytosis (histiocytosis X of bone). Cancer 1995;76:2471-2484
13. Al-Abbadi M, Masih A, Braylan RC, et al. Soft tissue Langerhans' cell histiocytosis in an adult. Arch Pathol Lab Med 1997;121:169-172
14. Schmitz L, Favara BE. Nosology and pathology of Langerhans cell histiocytosis. Hematol Oncol Clin North Am 1998;12:221-246
15. Brown RE. Angiotensin-converting enzyme, transforming growth factor β_1, and interleukin 11 in the osteolytic lesions of Langerhans cell histiocytosis. Arch Pathol Lab Med 2000;124:1287-1290
16. Huang F, Arceci R. The histiocytoses of infancy. Semin Perinatol 1999;23:319-331
17. Howarth DM, Gilchrist GS, Mullan BP, et al. Langerhans cell histiocytosis: diagnosis, natural history, management, and outcome. Cancer 1999;85:2278-2290
18. Egeler RM, D'Angio GJ. Langerhans cell histiocytosis. J Pediatr 1995;127:1-11
19. Huvos AG. Bone tumors. 2nd ed. Philadelphia: Saunders, 1991:695-771
20. Resnick D. Lipidoses, histiocytoses, and hypenlipoproteinemias. In: Resnick D, Niwayama G, eds. Diagnosis ofbone and joint disorders. Vol 4. 2nd ed. Philadelphia: Saunders, 1988;2429-2439
21. Prayer D, Grois N, Prosch H, Gadner H, Barkovich AJ. MR imaging presentation of intracranial disease associated with Langerhans cell histiocytosis. AJNR Am J Neuroradiol 2004;25:880-891
22. Azouz EM, Saigal G, Rodriguez MM, Podda A. Langerhans' cell histiocytosis: pathology, imaging and treatment of skeletal involvement. Pediatr Radiol 2005;35(2):103-15
23. Campanacci M. Bone and soft tissue tumors, 2nd ed. Springer, Berlin Heidelberg New York, 1999: 857-76
24. Dorfman HD, Czerniak B. Bone tumors. Mosby, St. Louis, Missouri, 1997:690-701
25. De Schepper AM, Ramon F, Van Marck E. MR imaging of eosinophilic granuloma: report of 11 cases. Skeletal Radiol 1993;22:163-6
26. Kilborn TN, Teh J, Goodman TR. Paediatric manifestations of Langerhans cell histiocytosis: a review of the clinical and radiological findings. Clin Radiol 2003;58(4):269-78
27. Keyaki A, Nabeshima S, Sato T, et al. Magnetic resonance imaging of calvarial eosinophilic granuloma with pericranial soft tissue reaction-case report. Neurol Med Chir (Tokyo) 2000;40:110-1
28. Wilner D. Radiology of bone tumors and allied disorders. Philadelphia: Saunders, 1982:1330-1435

대한자기공명의과학회지 13:74-80(2009)

두개골의 랑게르한스 세포 조직구증: 자기공명영상과 다른 영상과의 비교

[1]인하대학교 의과대학 영상의학과학교실, [2]성균관대학교 의과대학 삼성서울병원 영상의학과
[3]인하대학교 전자공학과, [4]한국외국어대학교 산업경영공학부

임수진[1] · 임명관[1] · 박선원[1] · 김정은[1] · 김지혜[2] · 김덕환[3] · 이석룡[4] · 서창해[1]

목적: 이 연구의 목적은 두개골 랑게르한스 세포 조직구증의 특징적인 자기공명 영상소견을 기술하고 단순촬영과 컴퓨터 단층 촬영에서의 영상소견과 비교함에 있다.

대상 및 방법: 총 9명의 환자 중 10예의 병변을 대상으로 자기공명 영상을 분석하였다(연령범위: 5-42세, 평균 연령: 18세, 전예 여자). 9예에서 수술이나 미세 침 흡입 생검술에 의해서 병리학적으로 두개골의 랑게르한스 세포 조직구증이 증명되었다. 모든 환자는 자기공명영상을 시행하였고 이 중 7명 (8예) 에서 컴퓨터 단층 촬영과 단순 촬영을 시행하였다. 두 명의 숙련된 신경영상의학 의사가 영상에서 병변의 위치, 크기, 모양과 특징을 독립적으로 분석하고 병변의 범위와 주변 조직으로의 침범 여부를 비교하였다.

결과: 병변은 모든 두개골에 편향 없이 분포하였다. 자기공명 영상에서 종괴들은 조영증강되는 골 융해성 종괴(10/10)로 주로 판사이 공간에 위치하고(8/10) 두피(9/10)나 경질막(7/10)을 침범하였다. 경질막의 조영증강(7/10)과 비후(4/10)가 모든 병변에서 보였다. 골 융해성 종괴의 크기는 1.1 cm에서 6.8 cm의 범위였으며 모양은 원형(5/10)이거나 난원형(5/10)이었다. 컴퓨터 단층 촬영에서 병변은 판사이 공간의 골 융해성 종괴로(6/8) 두피의 침범(7/8)이 잘 보였다. 컴퓨터 단층촬영에서 골미란이나 골파괴가 자기공명영상보다 좀 더 분명하게 보였지만 연부종괴와 경질막의 조영증강 유무는 판단하기 어려웠다. 이와 대조적으로 단순촬영에서 모든 랑게르한스 세포 조직구증은 도려낸 병터 (punched out) 모양(4/8)이나 beveled-edge 모양(4/8)의 골융해성 종괴로 보였고 두피나 경질막으로의 침범은 판단 할 수 없었다.

결론: 두개골 랑게르한스 세포 조직구증의 특징적인 자기공명 영상소견은 판사이 공간에 위치한 골 융해성 종괴가 경질막과 두피를 침범하는 것으로, 자기공명영상이 단순촬영이나 컴퓨터 단층 촬영 보다 우월한 영상 기법이다.

통신저자 : 임명관, (400-711) 인천시 중구 신흥동 3가 7-206, 인하대학교 의과대학 영상의학과학교실
Tel. 82-32-890-2769 Fax. 82-32-890-2743 E-mail: kanlim@inha.ac.kr